Scandinavian Journal of Forest Research

ISSN: 0282-7581 (Print) 1651-1891 (Online) Journal homepage: https://www.tandfonline.com/loi/sfor20

Uncertainties of mapping aboveground forest carbon due to plot locations using national forest inventory plot and remotely sensed data

Guangxing Wang , Maozhen Zhang , George Z. Gertner , Tonny Oyana , Ronald E. McRoberts & Hongli Ge

To cite this article: Guangxing Wang , Maozhen Zhang , George Z. Gertner , Tonny Oyana , Ronald E. McRoberts & Hongli Ge (2011) Uncertainties of mapping aboveground forest carbon due to plot locations using national forest inventory plot and remotely sensed data, Scandinavian Journal of Forest Research, 26:4, 360-373, DOI: 10.1080/02827581.2011.564204

To link to this article: https://doi.org/10.1080/02827581.2011.564204

Scandinavian Journal of Forest Research, 2011; 26: 360–373

Taylor & Francis
Taylor & Francis Group

ORIGINAL ARTICLE

Uncertainties of mapping aboveground forest carbon due to plot locations using national forest inventory plot and remotely sensed data

GUANGXING WANG[1], MAOZHEN ZHANG[2], GEORGE Z. GERTNER[3], TONNY OYANA[1], RONALD E. McROBERTS[4] & HONGLI GE[2]

[1]*Department of Geography and Environmental Resources, Southern Illinois University, Carbondale, IL, USA,* [2]*Department of Forest and Environmental Resources, Zhejiang A&F University, Zhejiang, China,* [3]*Department of Natural Resources and Environmental Sciences, University of Illinois at Urbana-Champaign, Urbana, IL, USA, and* [4]*Northern Research Station, U.S. Forest Service, St. Paul, MN, USA*

Abstract
Forest carbon sinks significantly contribute to mitigation of atmospheric concentrations of carbon dioxide. Thus, estimating forest carbon is becoming important to develop policies for mitigating climate change and trading carbon credits. However, a great challenge is how to quantify uncertainties in estimation of forest carbon. This study investigated uncertainties of mapping aboveground forest carbon due to location errors of sample plots for Lin-An County of China. National forest inventory plot data and Landsat TM images were combined using co-simulation algorithm. The findings show that randomly perturbing plot locations within 10 distance intervals statistically did not result in biased population mean predictions of aboveground forest carbon at a significant level of 0.05, but increased root mean square errors of the maps. The perturbations weakened spatial autocorrelation of aboveground forest carbon and its correlation with spectral variables. The perturbed distances of 800 m or less did not obviously change the spatial distribution of predicted values. However, when the perturbed distances were 1600 m or larger, the correlation coefficients of the predicted values from the perturbed locations with those from the true plot locations statistically did not significantly differ from zero at a level of 0.05 and the spatial distributions became random.

Keywords: *Aboveground forest carbon mapping, forest inventory, plot location error, remote sensing, simulation, uncertainty analysis.*

Introduction

Forests play a critical role in reducing carbon concentration in the atmosphere and mitigating global warming (Schimel et al., 2001; U.S. Climate Change Science Program, 2007). Thus, estimating forest vegetation carbon at national, regional, and global scales is becoming very important to develop policies for mitigating climate change and trading carbon credits in carbon market. Furthermore, managing and trading forest carbon at local scale requires its spatially explicit estimates (Corbera and Brown, 2008). There is a substantial literature in this area (Chen et al., 2000a, 2000b, 2003; Fang et al., 2002; Heath et al., 1996; Jarvis & Dewar, 1993; Kimball et al., 2000; Neilson et al., 2007; Peng et al., 2002; Running & Hunt, 1993; Smith & Heath, 2008; Tan et al., 2007; Wang et al., 2009; Woodbury et al., 2007). However, there are still many challenges to accurately map forest carbon and one of them relates to the amount of uncertainties contained in maps of quantified forest carbon.

Forest carbon consists of carbon pools in trunks, branches, leaves, ground vegetation, roots and soils, and can be divided into aboveground forest carbon and belowground root and soil carbon. However, most of the studies deal with aboveground forest carbon because this is a relatively large pool and other carbon pools can be obtained based on allometric equations. This study focuses on mapping carbon equivalent of aboveground tree biomass, including standing trees and deadwoods, but not stumps and ground vegetation. For simplification,

Correspondence: Guangxing Wang, Department of Geography and Environmental Resources, Southern Illinois University, 1000 Faner Drive, Carbondale, IL, USA. E-mail: gxwang@siu.edu

(*Received 27 January 2010; accepted 15 February 2011*)

ISSN 0282-7581 print/ISSN 1651-1891 online
DOI: 10.1080/02827581.2011.564204

the carbon equivalent was called aboveground forest carbon in this study. The widely used method to obtain spatially explicit estimates of aboveground forest carbon sinks is by combining forest inventory plot data with remotely sensed images, and then interpolating aboveground forest carbon from the sample plots to unobserved locations (Chen et al., 2003; Goward, et al., 1994; Kimball et al., 2000; Tan et al., 2007; Turner et al., 2003; Wang et al., 2009).

When the above method is used to map aboveground forest carbon, there are many sources of uncertainties, including biased sampling, plot location errors, measurement errors of tree variables (diameter and height), incorrect models on the relationship of volume with diameter and height, uncertainties from biomass and carbon conversion factors, sensor errors, uncertainties from geometrical and radiometric correction of remotely sensed data, and uncertainties on modeling the relationship of aboveground forest carbon with spectral composition, etc. The key to reducing the uncertainties is identifying their sources, modeling their accumulation and propagation, and finally quantifying the amount of uncertainties contributed to the final output. Wang et al. (2009) demonstrated a methodological framework for this purpose. The methodology included (1) developing an image-aided spatial co-simulation algorithm to combine national forest inventory plot data with Landsat TM images and generate the maps of aboveground forest carbon; (2) obtaining a polynomial regression model to establish the relationships of input uncertainties with output uncertainties; and (3) calculating relative uncertainty contributions from various input components to the output uncertainties to identify the main sources of input uncertainties.

The uncertainties of aboveground forest carbon estimates can be due to attribute errors, that is, the errors related to variables such as difference between a measurement of tree diameter and its truth, and location or position errors (Pontius, 2000, 2002). Several authors have studied the uncertainty in estimation and mapping of aboveground forest carbon stocks (Chen et al., 2000; Heath and Smith, 2000; Larocque et al., 2008; Nabuurs et al., 2008; Sierra et al., 2007; Wang et al., 2009). However, there are very few studies on the uncertainties of aboveground forest carbon sinks due to location errors of sample plots used for measurements of ground-based forest variables. This study will emphasize location errors of sample plots in the case of the co-use of remote sensing data and field data to map the aboveground forest carbon for standing trees and deadwoods. The aboveground forest carbon does not include the carbon from lying deadwood, soil, belowground biomass, litter, and biomass on the surface layer.

There are several sources of location errors. First of all, the location errors often take place due to incorrectly locating sample plots using global positioning system (GPS). Secondly, geometric correction for remotely sensed data and mismatching between image pixels and sample plots also cause location errors. These kinds of location errors are often random and vary depending on the equipment and technologies used, and are generally less than 100 m. Moreover, there are also intentional man-made plot location errors, for example, due to incorrect readings of coordinates from GPS and map grids. These errors are often large and easy to identify in the case of systematical sampling design. When random sampling design is used, these errors are unlimited and unpredictable.

A specific example for intentional man-made plot location errors is with the US Forest Inventory and Analysis (FIA) Program in which locations of sample plots are provided to the general public with random perturbations attached to them to obscure their actual locations (McRoberts et al., 2005). The perturbations are done centered at plot exact locations, and the radii of most perturbations are 800 m, with the maximum of 1600 m (that is, approximately one mile). The values of some plots are also swapped or exchanged with those plots within similar forest types. The criteria for the similarity vary regionally and include forest type group, stand characteristics (age, diameter, height, and density), and geographic proximity. The proportion of plots that are swapped is about 10%. This perturbation and swapping of plot locations is done by the US Forest Service FIA program to comply primarily with the policy for protecting the owner's privacy of private lands and properties (McRoberts et al., 2005). This example of man-made plot location errors takes place in the USA, but the idea behind it is generalized and can be applied to forest inventory programs, including China and other countries.

All types of location errors will result in uncertainties in aboveground forest carbon estimates obtained from maps. The uncertainties may be minor or very large depending on the amount of location errors; spatial variability and correlation of forest variables; estimation and mapping methods (design-based estimation vs. model-based estimation); spatial resolutions of the variables that are observed; forest area sizes; etc. The effects of location errors on estimation accuracy of aboveground forest carbon should be investigated in several ways: (1) at the population level, whether the uncertainties due to location errors have led to biased estimates of populations; (2) at the local level, whether the

uncertainties have resulted in biased estimates for each of unobserved locations; (3) whether spatial distributions of aboveground forest carbon estimates from the plots that have location errors have significantly differed from that of the true plot locations; (4) whether there is a threshold value for location errors over which both population and local estimates will be biased; and (5) if there is a threshold value, whether it is related to spatial resolutions of resulting maps of aboveground forest carbon.

For the research issues listed above, currently there are only a few reports published. For example, McRoberts et al., (2005) investigated the effects of perturbing and swapping FIA plot locations on estimation accuracy of forest variables in the USA and concluded that the effects were negligible for design-based estimates. This conclusion was also supported by Lister et al. (2005) and Guldin et al. (2005). Furthermore, they suggested that for model-based estimates, the effects differed depending on the estimation methods. The estimates were acceptable for kriging approaches, but unacceptable for regression approaches. This finding was consistent with that of Coulston et al. (2006), Guldin et al. (2005), McRoberts and Holden (2005). Moreover, Coulston et al. (2006) indicated that perturbing plot locations increased the nugget values of spatial autocorrelation-variogram models. In addition, Sabor et al. (2007) suggested that the impacts of location errors due to use of perturbed plots had a strong inverse relationship with mean map unit sizes of data-sets used in the analysis. They found that for a 30 m $\times$ 30 m resolution land cover map, the plot misclassification rate ranged from 32 to 66%, whereas for ecological subsection data with mean polygon size of 9067 km^2, the rate was only 1–10%.

This study investigated uncertainties of mapping aboveground forest carbon for standing trees and deadwoods due to location errors of sample plots. National forest inventory plot data and Landsat Thematic Mapper™ images were combined using sequential Gaussian co-simulation. The primary goals of this study are to (1) analyze the relationship of uncertainties of aboveground forest carbon predicted values with location errors of sample plots; (2) explore the impact of location errors on accuracy of population means, predicted values of local areas, and their spatial distribution and pattern; and (3) investigate whether there are threshold values of location errors that lead to biased population prediction and locally predicted values and their spatial distributions. It has to be pointed out that the aboveground forest carbon is the indirect result obtained by first converting the volumes of standing trees and deadwoods to biomass using biomass conversion coefficients or expansion factors and then to carbon using a standard carbon conversion factor.

Materials and methods

Study area

A case study was drawn from Li-An County, located in ZheJiang Province, a subtropical zone of East

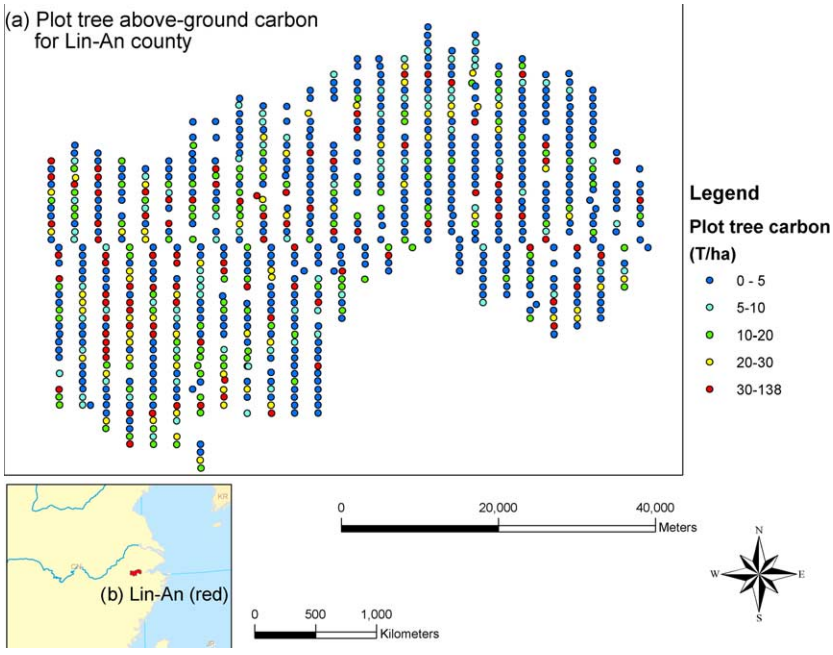

Figure 1. (a) Plot values of aboveground forest carbon in Lin-An County and (b) the location of the county within China.

China (Figure 1b), and is part of the China National Forest Inventory. Lin-An County has the latitudes from 29°56′N to 30°23′N and the longitudes from 118°51′E to 119°52′E with an area of 312,680 ha (Figure 1). Average annual temperature and precipitation are 16.4°C and 1628 mm. Mountainous areas dominate the county with an elevation range of 1770 m, and overall the elevation at the northwest is higher than at the southeast. Plantations dominate this area, and the typical forest ecosystems include coniferous forests, evergreen broad-leaf forests, deciduous and evergreen broad-leaf mixed forests, bamboo, shrubs, and fruit trees (Zhang et al., 2009).

China national forest inventory and permanent plots

In China, the national forest inventory was initiated in the 1950s (Fang et al., 2002). A systematic sample consisting of more than 250,000 plots was designed. Each of the sample plots represents areas from 1 km^2 to 64 km^2, and the plot sizes also varied depending on different forest regions (CMF-DFRM, 1996). The permanent plots have been re-measured at 5- or 10-year intervals.

The sample grid used for national forest inventory is 8 km × 8 km for Lin-An County. However, Lin-An local government added temporary forest inventory plots in 2004 and made a grid of 1 km × 3 km (Figure 1a). The sizes of the forest inventory plots are the same for both permanent and temporary plots: 28.3 m × 28.3 m (about 0.08 ha). In Lin-An County, there are a total of 50 permanent plots and 918 temporary plots available. However, a total of only 770 plots (i.e. 40 permanent plots and 730 temporary plots) were used in this study. The reason was that to cover Lin-An County, two scenes of Landsat TM images had to be acquired and merged, and to reduce the uncertainties due to merging of two scenes of images, the right scene covering the 770 plots was used in this study. The plot data were collected in 2004. The same methods were used to measure forest variables for both permanent and temporary plots. Within each plot, all trees were tallied and grouped into classes based on 2 cm diameter intervals, and then a sample tree for each class was randomly selected and measured for tree height.

Aboveground forest biomass and carbon

The volumes of individual trees within a plot, including stump but excluding branches, were calculated by species using the regression models used by national forest inventory program for this area (CMF-DFRM, 1996) and then summed to obtain estimates of plot tree volumes. Using biomass conversion coefficients (i.e. biomass expansion factors) from literature (Fang, 1999; Fang & Wu, 2006; Hu, 2007; Ma et al., 2007; Zhang, 1999; Zhang & Wang, 2008), the plot volumes were converted into forest biomass and aboveground forest carbon pools (trunk, branch, and leaf). The biomass conversion coefficient meant the total biomass obtained per cubic unit for tree volume. The carbon conversion factor used to convert forest biomass to carbon was 0.5.

Several authors have investigated the biomass conversion coefficients of the main tree species in this region (Fang, 1999; Fang & Wu, 2006; Hu, 2007; Ma et al., 2007; Zhang, 1999). In order to estimate the coefficients, more than 100 trees were sampled based on tree species groups (broad-leaf: hardwood and softwood, coniferous), age groups (young, middle-age, and mature), and different site conditions – slopes. At least three sample trees for each tree species group were obtained. The sample woods for different parts of each tree were then selected and dried. The resulting coefficients varied from 0.3067 to 0.6391 g/cm^{-3} depending on different species and species groups. The sample trees were grouped into broad-leaf and coniferous. The biomass conversion coefficients of broad-leaf trees ranged from 0.3067 to 0.4495 g/cm^{-3} and had a coefficient of variation of 15.9%. The biomass conversion coefficients of coniferous trees varied from 0.3640 to 0.6391 g/cm^{-3}, with a coefficient of variation of 9.7%. The broad-leaf trees were further divided into two sub-groups (softwood and hardwood) with average biomass conversion coefficients of 0.387 and 0.447 g/cm^{-3}. For coniferous trees, this study area was dominated by Chinese fir and Pinus Massoniana, and their average biomass conversion coefficients were 0.444 and 0.447 g/cm^{-3} and merged because of the similarity.

The biomass conversion coefficients were used to convert the volume of each tree to biomass. The biomass values of trees were then added to obtain forest biomass for each of the plots. The plot aboveground tree biomass values were converted to aboveground forest carbon. The spatial distributions of the plot aboveground forest carbon values are shown in Figure 1a and the unit used is tons per hectare (T/ha).

Landsat TM images

For Lin-An County, a Landsat Enhanced TM Plus (ETM+) scene covering 80% of the county and dated 3 August 2004 was acquired. The image consists of bands one to five and seven at a spatial resolution of 30 m × 30 m. The Universal Transverse Mercator (UTM) was used as reference coordinate

system, and the geometric correction of the image was done using a digital topographic map. The resulting root mean square error was less than one pixel. In addition to the original image bands, various band ratios were calculated. A band ratio was defined as one band or a group of bands divided by another band or another group of bands. The band ratios included

(1) Six inversions of bands: 1/TM1, 1/TM2, 1/TM3, 1/TM4, 1/TM5, and 1/TM7;
(2) Six simple band ratios: TM1/TM4, TM2/TM4, TM3/TM4, TM5/TM4, TM7/TM4, and TM8/TM4; and
(3) Four band group ratios: (TM4-TM3)/(TM4+TM3), (TM3+TM5)/TM7, (TM3+TM5+TM7)/TM4, and (TM2+TM3+TM5)/TM7.

In addition, principal component analysis of the original bands was also conducted based on correlation matrix. The desired goals for these image transformations were to reduce the dimensionality of the original image feature space; and to increase the Pearson product moment correlation of the spectral variables with aboveground forest carbon by reducing the redundant information due to high correlation between the bands and the effects of slopes and aspects on spectral reflectance.

Generating carbon maps

The study area was divided into a grid that consisted of equal size cells or pixels. Within the study area, the sample plot data were combined with Landsat ETM+ image data to generate a map of expected aboveground forest carbon. Aboveground forest carbon data were available only at the sample plots, while ETM+ image data existed everywhere within the area. Aboveground forest carbon maps were created using an image-aided sequential Gaussian co-simulation algorithm (Wang et al., 2009). In the algorithm it was assumed that aboveground forest carbon was a random process and its value at each location was a realization of this random process. The realization was created using the algorithm mentioned above. This algorithm had the following steps:

(1) A random path to visit each of the square cells or pixels mentioned above within the study area was set up, and a co-simulation program was then used to follow this path and create a realization of aboveground forest carbon at each pixel.
(2) A neighborhood in which plot data were used for prediction was determined based on the range of spatial autocorrelation of aboveground forest carbon will be mentioned below.
(3) At each pixel, the algorithm used the sample plot data, previously simulated values if any, and collocated image data within the given neighborhood to calculate a conditional mean and conditional variance by an unbiased collocated simple cokriging estimator will be described below.
(4) The conditional mean and variance were used to determine a conditional cumulative distribution function of aboveground forest carbon and from the distribution, a value was randomly drawn. This value was then regarded as a realization of aboveground forest carbon at this location and used as a conditional data for sequential simulation of neighboring locations.
(5) After all the pixels in the study area were visited and each of the pixels obtained a simulated value, the results represented a map for aboveground forest carbon. The process above was repeated multiple times, L, by setting up different random paths to visit each location across the study area, which resulted in a set of simulated values for each pixel. From the set of the simulated values, an E-type sample mean of aboveground forest carbon for each pixel was then calculated and used as a predicted value (Goovaerts, 1997).

The co-simulation algorithm was conditional on the sample data, previously simulated values and collocated image data, and led to the maps of aboveground forest carbon. The output maps had the similar spatial resolution to the sample plot under consideration and image pixel sizes, that is, 30 m $\times$ 30 m. Moreover, this algorithm is based on the spatial autocorrelation and cross correlation of variables, and unbiased cokriging estimator. The spatial autocorrelation also called spatial variability means that the closer the data locations, the more similar the data values of aboveground forest carbon Z. This feature can be characterized using variogram if an intrinsic hypothesis is met, that is, the increments $[Z(u) - Z(u+h)]$ of aboveground forest carbon are stationary of order two, meaning the expected difference between the values of the random process at two locations u and $u+h$ separated by the vector h is zero, and the variance of the difference is constant (Goovaerts, 1997, pp. 70–72).

The variogram can be then estimated using Equation 1 with plot data.

$$\hat{\gamma}_{zz}(h) = \frac{1}{2N(h)} \sum_{\alpha=1}^{N(h)} (z(u_\alpha) - z(u_\alpha + h))^2 \quad (1)$$

where $N(h)$ is the number of all the data location pairs separated by a separation vector h, called lag, $z(u_\alpha)$ and $z(u_\alpha + h)$ are data values of aboveground forest carbon at spatial locations u_α and $u_\alpha + h$, respectively. Given the intrinsically stationary assumption, the variogram is a function of h only and not a function of u. The sample variogram is then fitted using variance functions including spherical model – Equation 2, exponential and Gaussian models; and nested versions of these models.

$$\gamma^{Sph}(h) = \begin{cases} c_0 + c_1 \left[1.5\frac{h}{a} - 0.5\left(\frac{h}{a}\right)^3\right] & \text{if} \quad 0 < h \le a \\ c_0 + c_1 & \text{otherwise,} \end{cases} \quad (2)$$

where c_0 and c_1 are called nugget and structure parameters of the spherical model, and $c = c_0 + c_1$ is sill parameter. The nugget is the magnitude of the jump discontinuity at $h = 0$, implying micro variability. The structure and sill parameters account for structure and total variances of the spatial variability. a is range parameter defined as the distance at which the model value equals to the maximum sill and suggests the range of spatial dependence. Within the range, observations can be considered to be spatially dependent, and beyond the range, observations can be considered to be essentially independent. This range parameter was thus employed to determine the size of neighborhood in the co-simulation above.

On the other hand, it is also assumed that there is spatial cross correlation between the aboveground forest carbon Z and a spectral variable Y, implying a spatial linkage between these two variables and providing the basis on which the co-simulation algorithm can be used to generate the predicted values of aboveground forest carbon at unobserved locations using the sample plot data. The spatial cross correlation can also be estimated using a sample cross variogram from collocated sample data:

$$\hat{\gamma}_{zy}(h) = \frac{1}{2N(h)} \times \sum_{\alpha=1}^{N(h)} ((z(u_\alpha) - z(u_\alpha + h)(y(u_\alpha) - y(u_\alpha + h))), \quad (3)$$

where $y(u_\alpha)$ and $y(u_\alpha + h)$ are data values of spectral variable Y at spatial locations u_α and $u_\alpha + h$, respectively. In this study, the cross variogram was approximated by calculating the product of the variogram from aboveground forest carbon and the correlation coefficient between aboveground forest carbon and the spectral variable (Almeida & Journel, 1994). It has to be pointed out that for each of the simulation iterations mentioned above, the same variogram and cross variogram were used.

The unbiased collocated simple cokriging estimator was used to generate the conditional mean and conditional variance that determined a conditional cumulative distribution function of aboveground forest carbon for each pixel. The conditional mean was obtained by weighting the values of the plot aboveground forest carbon, previously simulated values if any, and collocated image data within the given neighborhood in Equation 4. The weights of the data varied depending on their distances to the location to be predicted and their spatial variability determined by the variogram mentioned above. Generally, the shorter the distance, the greater the weight of the data. At the same time, a conditional variance was calculated based on the spatial configuration of the used data and variograms in Equation 5.

$$z^{sck}(u) = \sum_{\alpha=1}^{n(u)} \lambda_\alpha^{sck}(u)[z(u_\alpha) - m_z] + \lambda_y^{sck}(u)[y(u) - m_y] + m_z \quad (4)$$

$$\sigma^{2(sck)}(u) = C_{zz}(0) - \sum_{\alpha=1}^{n(u)} \lambda_\alpha^{sck}(u) C_{zz}(u_\alpha - u) - \lambda_y^{sck}(u) C_{zy}(0) \quad (5)$$

where $z(u_\alpha)$ are the used sample data or previously simulated values at location α when location u is predicted, $\lambda_\alpha^{sck}(u)$ are the weights of the used sample data or previously simulated values at location α, $n(u)$ is the number of the sample data and previously simulated values, $\lambda_y^{sck}(u)$ is the weight of spectral data at collocated u, m_z is the mean of the sample data, and m_y is the mean of the spectral data. $C_{zz}(0)$ is the variance of aboveground forest carbon and $C_{zy}(0)$ is the covariance between aboveground forest carbon and spectral variable. When $h = u_\alpha - u$, $C_{zz}(h)$ is the covariance function of aboveground forest carbon. If the aboveground forest carbon is not only intrinsic stationary but also second-order stationary, that is, has both a constant mean and variance, then its covariance function exists and can be calculated using Equation 6 (Goovaerts, 1997, pp. 70–72):

$$C_{zz}(h) = C_{zz}(0) - \gamma_{zz}(h) \quad (6)$$

In order to determine the weights in the cokriging estimator, a system of equations has to be obtained by imposing the constraints of unbiased estimator and minimum variance of the error. This cokriging estimator is unbiased under the constraint: $\sum_{\alpha=1}^{n(u)} \lambda_{\alpha}^{sck}(u) + \lambda_{y}^{sck}(u) = 1$, implying that not all of the weights are zero and at least one data value must be used for prediction of each location.

The co-simulation algorithm possesses a feature that the predictions pass through the data points. That is, the data values at the sample locations should be honored. However, in this study this algorithm was modified so that the sample locations were predicted using the data-set from the true plot locations, and the obtained predicted values could be compared to those at the same locations using the data-sets from the perturbed plot locations based on the plot observations. Thus, it was possible to calculate root mean square errors between the plot values and predicted values.

In this study we further assumed that the aboveground forest carbon has a Gaussian distribution. In practice, we did not test the sample data for this distribution assumption. Instead, normal score transformation of all sample plot data and images was conducted before the simulation. Moreover, how many simulations should be run is another issue that deals with if the obtained result approached the expectation. As the number L of simulations increases, generally, the variance of predicted values across a study area rapidly decreases at the beginning and then slowly and eventually becomes stable. The number that leads to a stable map of aboveground forest carbon can be used. In this study, we investigated the relationship of the variance of predicted values across the study area with the number of simulations and found out that a number of 400 runs led to stable maps.

The above co-simulation algorithm differed from traditional cokriging. First of all, the collocated simple cokriging was not directly used to predict aboveground forest carbon at each pixel. Instead, it was used to generate a conditional mean and conditional variance to determine a conditional cumulative distribution function of aboveground forest carbon for each pixel. Secondly, in addition to the sample data, the previously simulated values and the collocated image data were employed. As mentioned above, moreover, this algorithm theoretically honors the data values at sample locations although in this study it was modified for comparison of the predicted values at the sample locations using the datasets from true and perturbed plot locations. In addition, it reproduces closely the declustered sample histogram, the covariance model of aboveground forest carbon Z, and cross covariance with spectral variable Y. Thus, the conditional simulation can overcome the smoothing of traditional cokriging and greatly help re-produce spatial variability of aboveground forest carbon (Goovaerts, 1997, pp. 369–389).

Design for perturbing plot locations and assessment of map uncertainty

In this study, locations of forest inventory plots were randomly moved within 10 different distance intervals including 5 m, 15 m, 30 m, 50 m, 100 m, 500 m, 800 m, 1600 m, 1600 m with plot values swapped, and 8000 m. Randomly moving the location of a plot within a given distance interval meant that the X- and Y-coordinates of the plot were changed, the amounts of the changes were determined using random numbers, and the maximum amount corresponded to the given distance interval. Furthermore, the change directions of the X- and Y-coordinates were determined by randomly choosing –1 and 1.

The perturbed distances were divided into two groups: equal to or smaller than 100 m and larger than 100 m. The first group of perturbed distances could be regarded as measurement errors of plot locations using global positioning system (GPS); and the mismatching of plot locations due to geo-referencing and registration errors when remotely sensed images are geo-referenced to a projected coordinate system. The second group of perturbed distances could be considered as occasional unintentional man-made errors such as misreading, recording mistakes; and the intentional moving of plot locations 1600 m, as done with the US FIA to comply with the policy for protecting private lands and properties information. For plots that were swapped, plot values of forest variables are swapped with those within the similar forest types. That is, plot values are exchanged between the plots within similar forest types in terms of tree species, age, diameter, height, and density. It has to be pointed out that in practice the plot location errors more than 100 m rarely take place. In this study, the random perturbation used in the US FIA program were used as an example of large plot location errors. The objective was to analyze the effect of extreme errors in plot locations on aboveground forest carbon mapping and to provide useful suggestions.

Perturbing the forest inventory sample plot locations within each of the distance intervals mentioned above led to 10 datasets. Using each of the datasets, the maps of aboveground forest carbon at the spatial resolution of 30 m $\times$ 30 m were generated using the co-simulation. It was assumed that the original plot locations were true locations. The aboveground

forest carbon maps obtained using each of the 10 data-sets from perturbed plot locations were compared to those using the data-set from the true plot locations. The comparisons were also done using 700 independent samples by randomly drawing pixels. The Pearson product moment correlation coefficients and root mean square error (RMSE) between the reference and predicted values of aboveground forest carbon were calculated. The accuracy of each of the maps obtained using the data-sets from both true and perturbed plot locations was also assessed by comparing the predicted values at the true plot locations with the field observations. When the data-set from the true plot locations was used, the aboveground forest carbon-predicted values at each of the true plot locations was generated by a cross validation procedure, that is, using the data of all the plots except for the location to be predicted. All the obtained correlation coefficients were statistically tested for their significant differences from zero using the equation $r_\alpha = \sqrt{t_\alpha^2/(n-2+t_\alpha^2)}$ based on the student's distribution at the level $\alpha = 5\%$, where n is the number of sample plots used.

Results

The sample datasets from the true and perturbed plot locations were used to calculate spatial variability or autocorrelation of aboveground forest carbon (T/ha). A spherical model was used to model spatial autocorrelation of the trends. The parameters of the estimated standardized variogram model are provided in Table I. As the perturbed distance of plot locations increased, the nugget parameter increased and the structure parameter decreased, but both slightly fluctuated for short distance perturbations. After the perturbed distance was larger than 100 m, the nugget parameter continuously increased up to 1.0 and the structure parameters decreased until reaching zero. The range parameter that indicated the maximum distance of spatial autocorrelation also increased. It has to be pointed out that overall the spatial autocorrelation of plot aboveground forest carbon was not very strong and had a large nugget parameter. The reason may be because of relatively large sampling distances between the plots.

The Pearson product moment correlation coefficients of plot aboveground forest carbon (T/ha) with 6 TM bands and their principal components and 16 band ratios were obtained. Because of space limit, most of the results were omitted, except for the correlation coefficients from the inversions of six original TM bands, and the best image was listed in Table II. The correlation coefficients varied from –0.2977 to 0.3521, and all of them statistically significantly differed from zero based on the critical value of 0.0758 at a significant level of 0.05 with 770 sample plots. The simple image transformations such as the inversions of original bands led to higher correlation than the original bands and the complicated transformations such as principal components. The inversions of TM1, TM2, TM3, and TM7 had higher correlation with aboveground forest carbon at the original plot locations than those of TM4 and TM5. Among a total of 28 images, plot aboveground forest carbon had the highest correlation with the band ratio 1/TM3.

When the plot locations were perturbed, the correlation coefficients using the best image were calculated and are also listed in Table II. As the perturbed distance of plot locations increased, overall the correlation coefficients decreased continuously (Table II). When the perturbed distance was equal to and less than 50 m, only a slight decrease of the correlation occurred. Larger decreases took

Table I. Standardized parameters of spherical models for spatial autocorrelation-variogram of plot aboveground forest carbon (T/ha). Goodness of fit is a measure for quantifying how well the model fits the sample data based on sum of square due to error and a value closer to 0 indicates a better fit. The number of the used plots was 770 for Lin-An County.

	Lin-An County			
Distance plot locations perturbed (m)	Nugget c_0	Structure c_1	Range a (km)	Goodness of fit
0	0.76	0.24	5.2	0.00320
5	0.84	0.16	9.2	0.00244
15	0.89	0.11	14.8	0.00127
30	0.88	0.12	16.0	0.00130
50	0.93	0.07	24.4	0.00080
100	0.89	0.11	20.0	0.00102
500	0.94	0.06	31.6	0.00045
800	0.92	0.08	27.4	0.00063
1600	1.00	0.00		0.00504
1600 with swap	1.00	0.00		0.00461
8000	1.00	0.00		0.00497

Table II. Pearson product moment correlation coefficients of plot aboveground forest carbon (T/ha) with spectral variables for Lin-An County (LA) for collocated true and perturbed plot locations and pixels. The number of the collocated plots used was 770.

	Correlation of aboveground forest carbon at original plot locations with inversions of six TM bands					
	1/TM1	1/TM2	1/TM3	1/TM4	1/TM5	1/TM7
LA correlation	0.2917*	0.3319*	0.3521*	0.1151*	0.2240*	0.2917*
Correlation of aboveground forest carbon at perturbed plot locations with 1/TM3 for Lin-An County						
	Distance plot locations perturbed (m)					
	0	5	15	30	50	100
LA correlation	0.3521*	0.3411*	0.3392*	0.3398*	0.3387*	0.2887*
	Distance plot locations perturbed (m)					
	500	800	1600	1600 with swap	8000	
LA correlation	0.1663*	0.1244*	0.03951	0.0320	0.04900	

Note: *indicating that the correlation coefficients were significantly different from zero at a significant level of 0.05

place when the perturbed distances increased from 50 to 100 m, from 100 to 500 m, and from 800 to 1600 m, respectively. In fact, when the perturbed distances were equal to and larger than 1600 m, the correlation coefficients of aboveground forest carbon with the spectral variables statistically became not significantly different from zero at a level of 0.05, that is, the correlation almost disappeared. The above results were expected, because the perturbation of sample plot locations diminished the spatial autocorrelation of aboveground forest carbon (Table I) and also weakened the Pearson product moment correlation of aboveground forest carbon with spectral variables for collocated locations (Table II).

The maps of aboveground forest carbon (T/ha) for Lin-An County were generated using the data-sets from true and perturbed plot locations (Figure 2a–g). When the data-set from the true plot locations was used, the co-simulation algorithm led to a map of aboveground forest carbon that had a similar spatial distribution of predicted values to that with the sample plot values (Figure 2a compared to Figure 1a). That is, overall the aboveground forest carbon had the largest predicted values in the north and west parts and the smallest predicted values in the east, south, and middle parts of the study area. The maps from the perturbed plot locations looked similar to that obtained from the true plot locations for the perturbed distances equal to and smaller than 800 m (Figure 2a–d). The maps from the perturbed distances of 5, 15, 30, and 50 m were obtained but omitted because they all looked similar. After the perturbed distances of 1600 m, the maps became totally random (Figure 2e–g). With the same perturbed distances of 1600 m, swapping plot values did not change the spatial distribution of the predicted values (Figure 2e and f).

The predicted values of aboveground forest carbon obtained using the field plot data from the original and perturbed plot locations (Figure 2a–g) were compared with the aboveground forest carbon observations at the original plot locations by calculating the root mean square errors (RMSE) (Table III). Overall the RMSE slightly fluctuated when the perturbed distance of plot locations increased up to 800 m and a dramatic increase of the RMSE occurred when the perturbed distances were equal to or larger than 1600 m. When the predicted values from the true plot locations were used as reference to compare the predicted values from the perturbed plot locations (Table IV), the Pearson product moment correlation coefficients decreased and the RMSEs increased as the perturbed distances increased. There were noticeable increases of the RMSEs when the perturbed distances increased from 30 to 50 m and from 100 to 500 m. Especially, the dramatic decrease of the correlation coefficients and the large increase of the RMSEs took place when the perturbed distances were equal to or larger than 1600 m. In fact, after the perturbed distance of 1600 m, the correlation coefficients statistically were not significantly different from zero at a significant level of 0.05.

In addition, the population means of predicted values for aboveground forest carbon obtained using the plot data from both true and perturbed plot locations were compared to the population parameters from the plot observations in Table V. Based on the prediction errors, the averages of predicted values were larger than that of the plot values when the perturbed plot locations were less than 100 m and after that smaller. However, all the averages of aboveground forest carbon predicted values from both true and perturbed plot locations fell into the confident interval (9.7566, 12.2090) calculated using the plot values and $\left(\bar{x}-\frac{t_\alpha S}{\sqrt{n-1}},\quad \bar{x}+\frac{t_\alpha S}{\sqrt{n-1}}\right)$ at a significant level of $\alpha = 0.05$, where $\bar{x}$ and S were the mean and standard deviation from the plots observations, and $n=770$ was the number of plots.

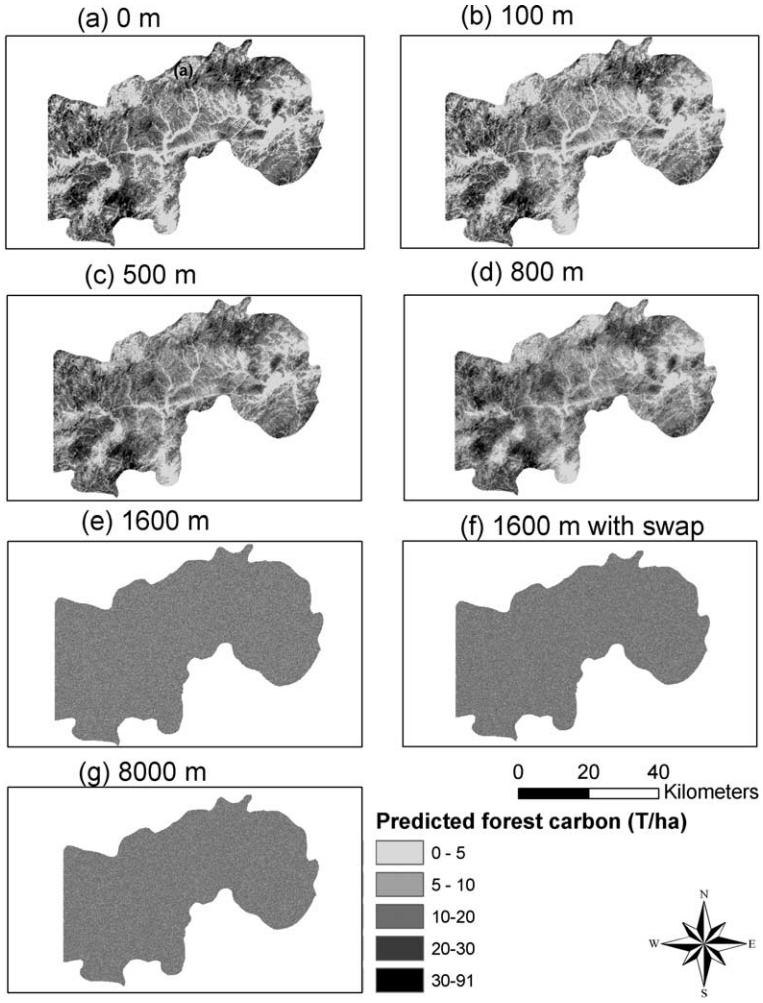

Figure 2. For Li-An County, spatial distributions of predicted values of aboveground forest carbon obtained with the data-sets from (a) true plot locations; and perturbed plot locations with distance of (b) 100 m, (c) 500 m, (d) 800 m, (e) 1600 m, (f) 1600 m with swapped plots values, and (g) 8000 m. The size of output map units was consistent with plot and pixel size: 30 m × 30 m.

Discussion

This study concentrated on investigating the uncertainties due to location errors of sample plots that were used to generate aboveground forest carbon maps and led to the following conclusions:

(1) The sequential Gaussian co-simulation used in this study led to the aboveground forest carbon predicted values that had similar spatial distribution to the observations of plots when the perturbed distances of plot locations were equal to and less than 800 m.
(2) All the perturbations of the plot locations statistically did not lead to biased population mean predictions of aboveground forest carbon based on the confidence interval calculated using the plot values at a significant level of

Table III. The root mean square errors (RMSE) when the predicted values of aboveground forest carbon (T/ha) obtained from both true and perturbed plot locations were compared with the observations of 770 plots in Lin-An (LA) County. The size of output map units was consistent with plot and pixel sizes: 30m × 30m.

	Distance plot locations perturbed (m)					
	0	5	15	30	50	100
LA RMSE	12.9514	12.5613	12.6994	12.6403	12.7718	12.4968
	Distance plot locations perturbed (m)					
	500	800	1600	1600 with swap	8000	
LA RMSE	12.7056	12.9109	14.3620	14.4872	14.3459	

Table IV. The Pearson product moment correlation coefficients and root mean square errors (RMSE) when the predicted values of aboveground forest carbon (T/ha) obtained using the field plot data from perturbed plot locations were compared with those from true plot locations using 700 independently sampled pixels for Lin-An County. The size of output map units was consistent with plot and pixel sizes: 30m × 30m.

	Distance plot locations perturbed (m)				
	5	15	30	50	100
LA correlation	0.9168*	0.9033*	0.9053*	0.8853*	0.8960*
LA RMSE	5.2401	5.6894	5.6590	6.2148	6.3219
	Distance plot locations perturbed (m)				
	500	800	1600	1600 with swap	8000
LA correlation	0.7953*	0.7631*	0.0417	0.0396	0.0391
LA RMSE	8.8632	9.1685	12.4147	12.5609	12.3682

Note: *indicating that the correlation coefficients were significantly different from zero at a significant level of 0.05

0.05. But, the perturbations resulted in positive prediction errors for the perturbed distances equal to and less than 100 m and the negative prediction errors for the perturbed distances larger than 100 m. Moreover, the perturbations obviously increased the root mean square error (RMSEs) of the spatially predicted values. The larger the perturbed distances of plot locations, the larger the RMSE. The perturbed distances equal to or larger than 1600 m would dramatically increased the RMSE.

(3) Perturbations of the plot locations weakened the Pearson product moment correlation of aboveground forest carbon with spectral variables and also had an influence on spatial autocorrelation of aboveground forest carbon by increasing the nugget and range parameters of the variogram model and decreasing its structure parameter. The larger the perturbed distances of plot locations, the greater the increase in the nugget and range parameter and reduction in the structure parameter. The perturbed distances equal to or larger than 1600 m would result in the disappearance of the spatial autocorrelation and Pearson product moment correlation.

(4) The perturbed distances of plot locations from 5 m to 800 m did not result in different spatial distributions of aboveground forest carbon-predicted values compared to that from the true locations. That is, small and moderate amounts of plot position errors, for example, the errors using GPS to locate plots and conduct geometric correction of images, generally, will not lead to noticeably different spatial distributions of aboveground forest carbon-predicted values.

(5) The perturbed distances of plot locations equal to or larger than 1600 m led to a randomly spatial distributions of aboveground forest carbon-predicted values. Swapping plot values may slightly increase the Pearson product moment correlation of aboveground forest carbon with spectral variables, but did not change the quality of the maps compared to that without swapping.

Because there are many sources of errors, quantifying the uncertainties for mapping aboveground forest carbon is still a great challenge. This study focused on investigating the uncertainties due to plot location errors and their effects on spatially predicted values and their spatial distributions of aboveground forest carbon. The plot location errors considered in this study meant the differences of plot X- and Y-coordinates from true locations, including plot positioning errors when sample plots are located using GPS, misreadings of X- and

Table V. The population averages of predicted values for aboveground forest carbon (T/ha) and their errors obtained from both true and perturbed plot locations based on the observations of $n = 770$ plots in Lin-An (LA) County when the size of output map units was consistent with plot and pixel sizes. The mean $\bar{x}$ and standard deviation s from the observations were 10.9828 and 17.3486 with a confident interval (9.7566, 12.2090) calculated using $\left(\bar{x} - \frac{t_\alpha S}{\sqrt{n-1}}, \quad \bar{x} + \frac{t_\alpha S}{\sqrt{n-1}}\right)$ at a significant level of $\alpha = 0.05$.

	Distance plot locations perturbed (m)					
	0	5	15	30	50	100
LA PE	12.0509	11.9239	11.6317	11.7331	11.3683	11.3292
LA error	1.0681	0.9411	0.6489	0.7503	0.4035	0.3464
	Distance plot locations perturbed (m)					
	500	800	1600	1600 with swap	8000	
LA PE	10.5646	10.5115	9.9240	9.3385	10.1159	
LA error	−0.4182	−0.4713	−1.0588	−1.6223	−0.8669	

Y-coordinates, location errors due to mismatching the sample plots with image pixels, etc. Moreover, intentionally perturbed plot locations for protection of private properties in the US forest inventory and analysis program was also involved in this study. However, the location errors and their effects on the results of aboveground forest carbon are difficult to separate. For this purpose, a further study is needed.

More important is that because of space limitation, this study neglected other sources of errors and uncertainties such as measurement and sampling errors of tree variables (diameter, height, etc.), uncertainties on the used relationships of tree diameter and height with volumes, sensor errors, and uncertainties due to knowledge gaps, etc. (Gonzalez et al., 2010; Larocque et al., 2008; Nabuurs et al., 2008; Phillips et al., 2000). Based on Nabuurs et al. (2008), the uncertainty of estimating aboveground forest carbon often is very high, much higher than the change to be achieved in carbon sequestration through changes in forest management. Phillips et al. (2000) pointed out that the recognized error components were sampling error for sample plot selection and measurement error for tree height and diameter, and regression error for tree volume. Nabuurs et al. (2008) implied that the stem model parameters mainly determined the output of aboveground forest carbon.

Gonzalez et al. (2010) estimated five aboveground carbon pools (live trees, dead trees, shrubs, coarse woody debris, and litter) and concluded that Lidar and QuickBird detected aboveground carbon in live trees, 70–97% of the total and Lidar showed lower uncertainty than QuickBird, due to high correlation of biomass to height and undercounting of trees by the crown detection algorithm. Wang et al. (2009) found out that the variation of image data had more impact on the accuracy of aboveground forest carbon-predicted values than the sample plot data.

Moreover, in this study the aboveground forest carbon was obtained by converting tree volumes to biomass and then to carbon using the biomass conversion coefficients or expansion factors and standard carbon conversion factor. In fact, the conversion factors greatly vary depending on tree species, environment in which trees grow, and methods by which the factors are obtained. For example, the biomass conversion factors used in this study had a variation coefficient 15.9%. Another example is the finding of Tolunay (2009) that in northwestern Turkey the carbon conversion factor was 0.53, 0.53, 0.50, and 0.40 for aboveground trees, needles, floor litter, and humus layer, respectively. Without doubt, the variability and uncertainties of the conversion factors can greatly affect the accuracy of the aboveground forest carbon-predicted values. In addition, the aboveground forest carbon mapped in this study did not include the carbon from lying deadwoods, soil, belowground biomass, litter, and biomass on the surface layer. Thus, the uncertainties in respect to the sources were neglected.

In addition, the sample grid used in this study was 1 km × 3 km. The relatively large distances between the sample plots led to the difficulties to calculate the sample variogram and cross variogram and further became a source of uncertainty for mapping the aboveground forest carbon. On the other hand, capturing the characteristics of the variograms also depends on the complexity of forest landscapes. In this study, the spatially adjacent plantations dominated Lin-An County, and the forests had similar structures in ages, tree species, and canopies. The forest landscapes thus were relatively simple. Therefore, the relatively large sample grid did not seriously impede the derivation of the sample variograms.

Acknowledgements

Funding for this study was in part supported by Dr Wang's startup from Southern Illinois University Carbondale and the National Natural Science Foundation of China (No#: 30972360). We also would like to thank the editor and reviewers.

References

Almeida, A. S. & Journel, A. G. (1994). Joint simulation of multiple variables with a Markov-Type coregionalization model. *Mathematical Geology*, *26*, 565–588.

Chen, J. M., Chen, W., Liu, J. & Cihlar, J. (2000). Annual carbon balance of Canada's forests during 1895–1996. *Global Biogeochemical Cycle*, *14*(3), 839–850.

Chen, W. J., Chen, J. M., Liu, J. & Cihlar, J. (2000). Approaches for reducing uncertainties in regional aboveground forest carbon balance. *Global Biogeochemical Cycle*, *14*(3), 827–838.

Chen, J. M., Ju, W., Cihlar, J., Price, D., Liu, J., Chen, W., et al. (2003). Spatial distribution of carbon sources and sinks in Canada's forests based on remote sensing. *Tellus B*, *55*(2), 622–642.

Chinese Ministry of Forestry-Department of Forest Resource and Management CMF-DFRM. (1996). *Forest resources of China 1949–93*. Liu-hai-hu-tong 7. Beijing: Chinese Forestry Press.

Corbera, E. & Brown, K. (2008). Building institutions to trade ecosystem service; marketing aboveground forest carbon in Mexico. *World Development*, *36*(10), 1956–1979.

Coulston, J. W., Riitters, K. H., McRoberts, R. E., Reams, G. A. & Smith, W. D. (2006). True versus perturbed forest inventory plot locations for modeling: A simulation study. *Canadian Journal of Forest Research*, *36*, 801–807.

Fang, J., Chen, A., Peng, C., Zhao, S. & Ci, L. (2002). Changes in forest biomass carbon storage in China between 1949 and 1998. *Science*, *292*, 2320–2322.

Fang, W. & Wu, Y. (2006). A study on the rate of hardwood tissue. *Journal of Fujian College of Forestry*, *26*(3), 224–228.

Fang, Y. (1999). Variation of wood gravity for *Pinus Massoniana* plantations. *Forestry Science and Technology*, *6*, 37.

Gonzalez, P., Asner, G. P., Battles, J. J., Lefsky, M. A., Waring, K. M. & Palace, M. (2010). Aboveground forest carbon densities and uncertainties from Lidar, QuickBird, and field measurements in California. *Remote Sensing of Environment*, *114*(7), 1561–1575.

Goovaerts, P. (1997). *Geostatistics for natural resources evaluation*. New York: Oxford University Press.

Goward, S. N., Waring, R. H., Dye, D. G. & Yang, J. (1994). Ecological remote sensing at OTTER: Satellite macroscale observations. *Ecological Applications*, *4*, 322–343.

Guldin, R. W., King, S. I. & Scott, C. T. (2005). Vision for the future of FIA: Pacan to Progress, possibilities, and partners. In R. E. McRoberts, G. A. Reams, P. C. Van Deusen & W. H. McWilliams (Eds.), Proceedings. Of the 6th annual forest inventory and analysis symposium,. USDA For. Ser. Gen. Tech. Rep. WO-GTR-70. Wasington, DC: USDA Forest Service.

Heath, L. S., Birdsey, R. A., Row, C. & Plantinga, A. J. (1996). Carbon pools and flux in forest products. In: M. J. Apps and D. T. Price (Eds.) Forest Ecosystems, Forest Management, and the Global Carbon Cycle. NATO ASI Series I: *Global Environmental Changes*, *40*, 271–278.

Heath, L. S. & Smith, J. E. (2000). An assessment of uncertainty in aboveground forest carbon budget projections. *Environmental Science and Policy*, *3*, 73–82.

Hu, J. (2007). The study on the clone selection and assessment for the seed orchard of *Pinus massoniana*. *Journal of Fujian Forestry Science and Technology*, *34*(2), 32–35.

Jarvis, P. G. & Dewar, R. C. (1993). Forests in the global carbon balance: From stand to region. In J. R. Ehleringer and C. B. Field (Eds.), *Scaling physiological processes: leaf to globe* (pp. 191–222). San Diego, CA: Academic Press.

Kimball, J. S., Keyser, A. R., Running, S. W. & Saatch, S. S. (2000). Regional assessment of boreal forest productivity using an ecological process model and remote sensing parameter maps. *Tree Physiology*, *20*, 761–775.

Larocque, G. R., Bhatti, J. S., Boutin, R. & Chertov, O. (2008). Uncertainty analysis in carbon cycle models of forest ecosystems: Research needs and development of a theoretical framework to estimate error propagation. *Ecological Modelling*, *219*, 400–412.

Lister, A., Scott, C. T., King, S. L., Hoppus, M., Butler, B. & Griffith, D. (2005). Strategies for preserving owner privacy in the national information management system of the USDA Forest Service's forest inventory and analysis unit. In R. E. McRoberts, G. A. Reams, P. C. Van Deusen & W. H. McWilliams (Eds) *Proceedings of the Fourth Annual Forest Inventory and Analysis Symposium*, pp. 163–166. 19–21 November, 2002, New Orleans, La. USDA For. Serv. Gen. Tech. Rep. NC-252. Saint Paul, MN: USDA Forest Service and North Central Research Station.

Ma, Z., Liu, Q., Xu, W., Li, X. & Liu, Y. (2007). Carbon Storage of Artificial Forest in Qianyanzhou,Jiangxi Province. *Scientia Silvae Sinicae*, *43*(11), 1–7.

McRoberts, R. E., Holden, G. R., Nelson, M. D., Liknes, G. C., Moser, W. K., Lister, A. J., et al. (2005). Estimating and circumventing the effects of perturbing and swapping inventory plot locations. *Journal of Forestry*, *103*, 275–279.

McRoberts, R. E. & Holden, G. H. (2005). Evaluating the effect of uncertainty in inventory plot locations. Sustainable forestry in theory and in practice, recent advances in inventory and monitoring, statistics and modeling, information and knowledge management, and policy science. In Reynolds, K., K. Rennolls, A. Thomson, M. Shannon, and M. Kohl (Eds.). Proceedings. Of the IUFRO meeting, April 5–8, 2005, Edinburgh, Scotland, Gen. Tech. Rep. USDA Forest Services, Portland, OR. Pacific Northwest Research Station. Portland, OR: USDA Forest Service and Pacific Northwest Research Station.

Nabuurs, G. J., Van Putten, B., Knippers, T. S. & Mohren, G. M. J. (2008). Comparison of uncertainties in carbon sequestration estimates for a tropical and a temperate forest. *Forest Ecology and Management*, *256*, 237–245.

Neilson, E. T, MacLean, D. A., Meng, F. R., Meng, F. R. & Arp, P. A. (2007). Spatial distribution of carbon in natural and managed stands in an industrial forest in New Brunswick, Canada. *Forest Ecology and Management*, *253*(1), 148–160.

Peng, C., Liu, J., Dang, Q., Apps, M. J. & Jiang, H. (2002). TRIPLEX: A generic hybrid model for predicting forest growth and carbon and nitrogen dynamics. *Ecological Modelling*, *153*, 109–130.

Phillips, D. L., Brown, S. L., Schroeder, P. E. & Birdsey, R. A. (2000). Toward error analysis of large-scale aboveground forest carbon budgets. *Global Ecology & Biogeography*, *9*(4), 305–313.

Pontius, R. G. (2000). Quantification error versus location error in comparison of categorical maps. *Photogrammetric Engineering and Remote Sensing*, *66*(8), 1011–1016.

Pontius, R. G. (2002). Statistical methods to partition effects of quantity and location during comparison of categorical maps at multiple resolutions. *Photogrammetric Engineering and Remote Sensing*, *68*(10), 1041–1049.

Running, S. W. & Hunt, E. R. Jr. (1993). Generalization of a forest ecosystem process model for other biomes, BIOME-BGC, and an application for global scale models. In J. R. Ehleringer & C. B. Field (Eds.), *Scaling physiological processes: leaf to globe* (pp. 141–158). San Diego, CA. Academic Press.

Sabor, A. A., Radeloff, V. C., McRoberts, R. E., Clayton, M. & Stewart, S. I.(2007). Adding uncertainty to forest inventory plot locations: effects on analyses using geospatial data. *Canadian Journal of Forest Research*, *37*, 2313–2325.

Schimel, D. S., House, J. I., Hibbard, K. A., Bousquet, P., Ciais, P., Peylin, P., et al. (2001). Recent patterns and mechanism of carbon exchange by terrestrial ecosystems. *Nature*, *414*, 169–172.

Sierra, C. A., Valle, J. I., Orrego, S. A., Moreno, F. H., Harmon, M. E., Zapata, M., et al. (2007). Total carbon stocks in a tropical forest landscape of the Porce region, Colombia. *Forest Ecology and Management*, *243*, 299–309.

Smith, J. E. & Heath, L. S. (2008). *Carbon Stocks and Stock Changes in U.S. Forests and Appendix C. In U.S. Agriculture and Forestry Greenhouse Gas Inventory: 1990–2005. Global Change Program Office, Office of the Chief Economist*. (pp. 65–80). Technical Bulletin No. 1921. http://www.usda.gov/oce/global_change/AFGGInventory1990_2005.htm

Tan, K., Piao, S., Peng, C. & Fang, J. (2007). Satellite-based estimation of biomass carbon stocks for northeast China's forests between 1982 and 1999. *Forest Ecology and Management*, *240*, 114–121.

Tolunay, D. (2009). Carbon concentrations of tree components, forest floor and understory in young Pinus sylvestris stands in north-western Turkey. *Scandinavian Journal of Forest Research*, *24*(5), 394–402.

Turner, D. P., Ritts, W. D., Cohen, W. B., Gower, S. T., Zhao, M., Running, S. W., et al. (2003). Scaling gross primary production (GPP) over boreal and deciduous forest landscapes in support of MODIS GPP product validation. *Remote Sensing of Environment*, *88*, 256–270.

US Climate Change Science Program. (2007). *The North American carbon budget and implications for the global carbon cycle*.

Retrieved November 13, 2007, from http://www.climatescience.gov/ Library/sap/sap2-2/final-report/default.htm.

Wang, G., Oyana, T., Zhang, M., Adu-Prah, S., Zeng, S., Lin, H., et al. (2009). Mapping and spatial uncertainty analysis of forest vegetation carbon by combining national forest inventory data and satellite images. *Forest Ecology and Management*, *258*(7), 1275–1283.

Woodbury, P. B., Smith, J. E. & Heath, L. S. (2007). Carbon sequestration in the US forest sector from 1990 to 2010. *Forest Ecology and Management*, *241*, 14–27.

Zhang, M. & Wang, G. (2008). The forest biomass dynamics of Zhejiang Province. *Acta Ecologica Sinica*, *28*(11), 5665–5674. (in Chinese, Abstract in English).

Zhang, M., Wang, G., Zhou, G., Ge, H., Xu, L. & Zhou, Y. (2009). Mapping of forest carbon by combining forest inventory data and satellite images with co-simulation based up-scaling method. *Acta Ecologica Sinica 29*(6), 2919–2928. (in Chinese, Abstract in English).

Zhang, Y. (1999). Measuring gravities and pulpwood rates of poplar species. *Journal of Liaoning Forestry Science & Technology*, *2*, 50–51.